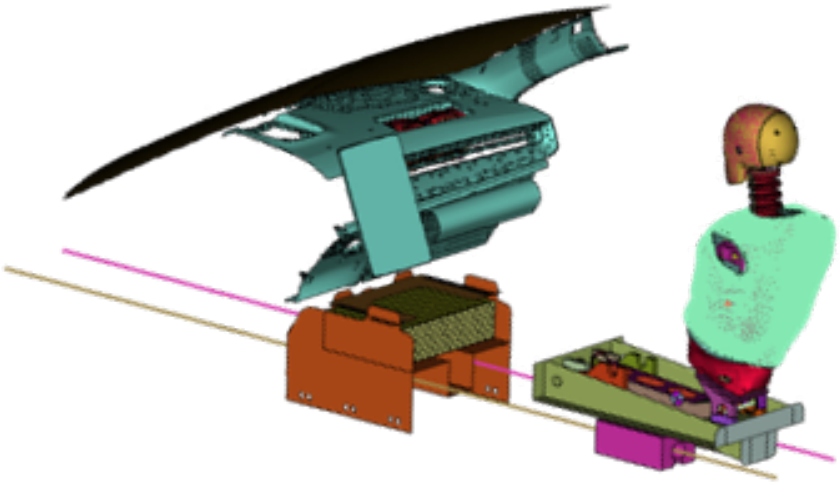

Redesign of dummy impact system test

NITIN DAVANGERE ANAND
PRIYATHAM REDDY KARETI

Department of Mechanics and Maritime Sciences
Chalmers University of Technology
Gothenburg, Sweden 2022

Redesign of dummy impact system test

Nitin Davangere Anand
Priyatham Reddy Kareti

Master's thesis in mechanics and maritime sciences - MMSX30 2022: 51
Supervisors: Robert Landholm and Stefan Ask
Examiner: Robert Thomson
CHALMERS UNIVERSITY OF TECHNOLOGY
SE-412 96 Gothenburg
Sweden
Nr: +46 (0)31-772 1000

Cover: Airbag component test setup
Typeset in LaTeX
Gothenburg, Sweden 2022

Redesign of dummy impact system test
PRIYATHAM REDDY KARETI
NITIN DAVANGERE ANAND

Department of Mechanics and Maritime Sciences
Chalmers University of Technology

Abstract

With the need for testing airbags for unbelted passenger crash scenarios, a component test setup was developed to test the passenger side airbags for the USNCAP FFRB 25 mph 50th percentile unbelted load case. This test setup simulates the physics of a frontal vehicle car crash while mimicking the kinematics of a dummy loading into the airbag. Honeycomb (HC) is used to decelerate the sled that holds the dummy interacting with the airbag. Although the HC achieves the deceleration target with a good strength-to-weight ratio, it is plastically deformed and must be discarded after each test. The purpose of this thesis is to find an alternate deceleration feature that can make the test setup configuration repeatable and robust for different load cases, thus broadening the scope of the test setup. A comparative study was conducted on different deceleration features and a damper system proved to be a good alternate to the HC when assessed with design criterias. This damper system was incorporated into the existing Computer-Aided Engineering (CAE) model, which is closely validated to the test setup using the finite element method. This report explores designing a damper with a discrete element feature available in LS DYNA, and parameter studies were conducted to understand the damper behaviour. A simplified model was built that could reproduce the physics of the crash configuration to understand the discrete element characteristic with multiple iterations. Later the finalised damper was incorporated into the full scale CAE model by replacing the honeycomb. The findings of this thesis will be useful to the industry in the future when designing a damper for various load conditions using Finite Element Analysis (FEA) in the LS DYNA platform.

Keywords: Component test rig, Damper modelling, Crash deceleration feature, LS DYNA, Finite element

Contents

1 Introduction

1.1 Background

According to the National Highway Traffic Safety Administration (NHTSA), frontal airbags saved 50,457 lives in the United States alone between 1987 and 2017 [1]. Due to the deployment of frontal airbags, driver fatalities are reduced by 29% and passenger fatalities are reduced by 32% for those aged 13 and above [2]. Despite the fact that safety standards are improving year after year around the world, accidents involving unbelted passengers continue to prevail. In most car accidents, the deployment of airbags is critical to prevent serious injuries to the occupants. Early deployment of the airbag produces a firm cushioning effect, whereas late deployment produces a low stiffness, causing the occupant to collide with the vehicle's stiffer elements, such as steering wheel or dashboard, resulting in an injury. With today's computing capacity, multiple airbag deployments may be tested using CAE methodologies to anticipate injury to an occupant in a variety of load conditions. Though the findings of modern CAE techniques are near to forecasting reality, validations must be carried out using physical crash tests.

Setting up a full frontal crash test is expensive and time-consuming, and involving a full car crash just for airbag testing, is not beneficial to the corporation. To address this issue, an airbag component test setup was built to test airbags at a cheaper cost. The test setup validates the airbag by evaluating the head and neck injury criterias on a Half dummy (HD). The lower torso of the HD is attached to the sled, and limbs are neglected as the focus is only on the head and chest interactions with the airbag. In the testing of passenger airbag (PAB) for unbelted load cases, the torso and head of the human body dummy is accelerated up to a certain speed towards the instrument panel (IP) of the car. This requires a controlled deceleration during the test phase from the airbag component and the test equipment, working together. The deceleration of the sled is achieved by an aluminum honeycomb (HC) block placed in an anvil, under the instrument panel. The HD interacts with the airbag and the HC decelerates the sled that the HD is attached to. This test setup represents the dynamics of a frontal collision impact of a car. The component test setup used for testing airbag is shown in Figure 1.

Figure 1: Test setup for testing PAB

Although the HC is good enough to decelerate the sled at a controlled rate, it has few major drawbacks. In the current test setup, the aluminum HC block can be used only once as it undergoes plastic deformation during each test. The manual work of cutting the HC blocks to precise measurements for each test is not feasible as there are irregularities on the edges of the block as seen in Figure 4. This leads to misalignment in positioning of the HC block inside the anvil. Figure 2 shows that the velocity profiles of the sled for different tests conducted. The steps observed in Figure 2 could be the required crash pulse in the test or it could be due to crushing of the HC block in different stages or could be due to movement of the HC block between the anvil and the sled leading to more contact friction opposing the sled. From Figure 3 it can be noticed that for tests with impact velocity greater than 12 m/s, a huge peak in acceleration upto 1200 m/s^2 is obtained. This means that the HC block has bottomed out and is unable to absorb the energy from the sled. The dimensions of the aluminum HC used in the current test setup are $378 \times 247 \times 96$ mm $(l \times b \times h)$.

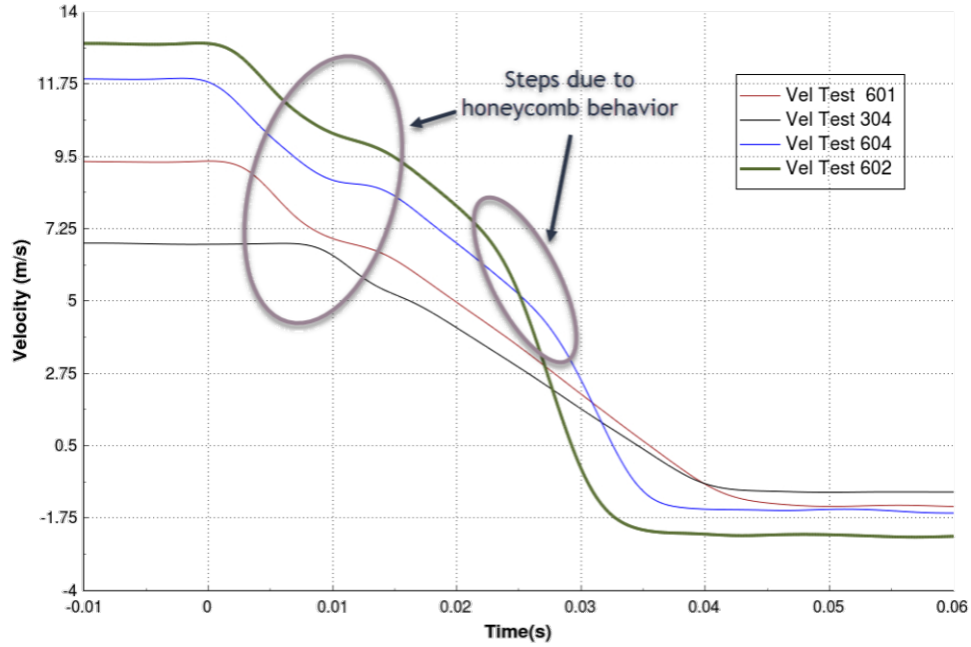

Figure 2: Velocity of sled due to HC

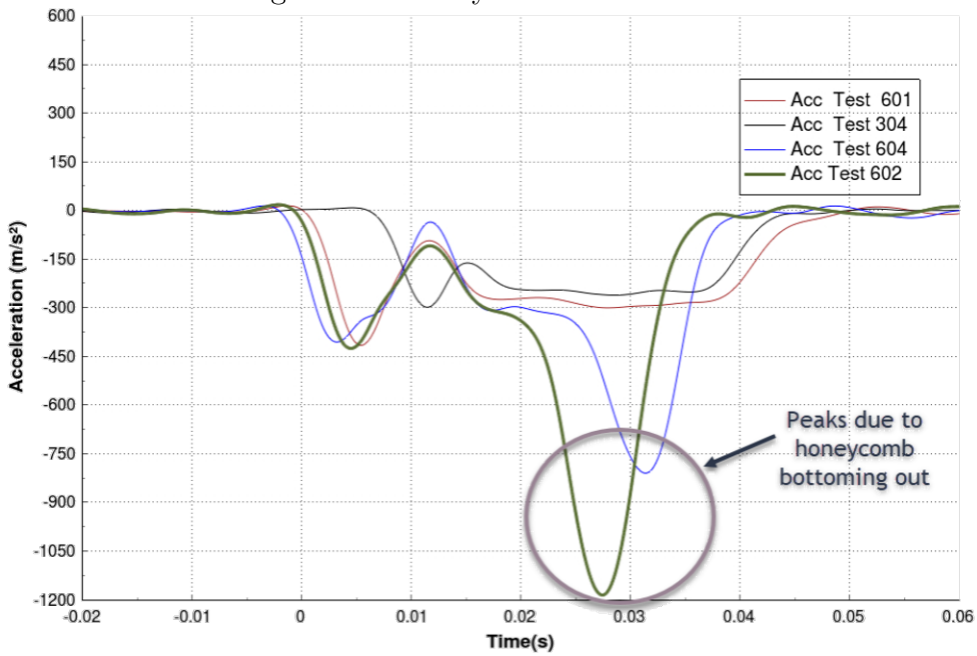

Figure 3: Acceleration of sled due to HC

Different crash pulses can be created by altering the stiffness of the HC block by varying the cell size as shown in Figure 5.It is not feasible for the industry to purchase HC with different properties for various tests. The current HC block used in the crash test setup has around 18-20 pores per 9 cm of length. Various HC blocks were tested previously from 8 - 10 pores per 9 cm of length to 24-25 pores per 9 cm of length.

Figure 4: HC used in test setup

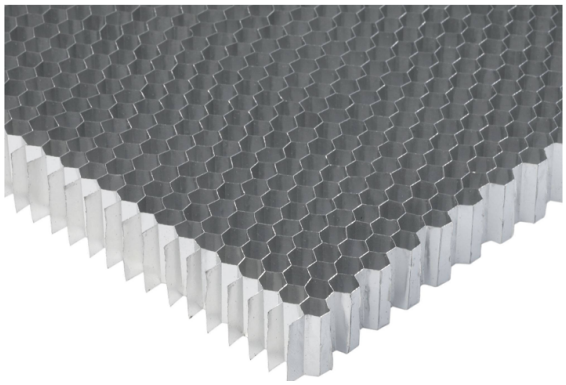

(a) fine pores

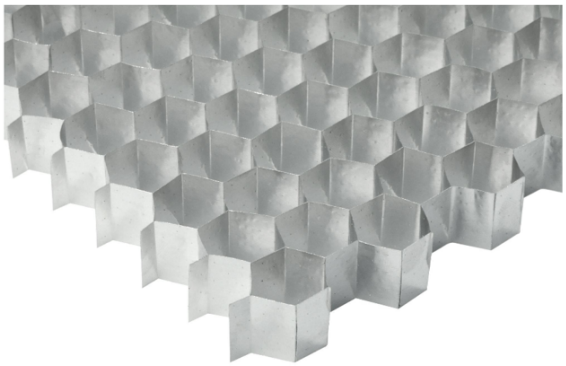

(b) course pores

Figure 5: HC with various cell sizes in market [3]

The test setup when used with HC is not robust and does not deliver repeatable results. The crushed HC block also leads to aluminum waste which is unsustainable for the industry.

1.2 Objective

The objective of the thesis is to propose a suitable system of deceleration technique that could replace the HC block and replicate an existing crash test result as shown in Figure 12. The initial task of the thesis was to select an ideal result from the existing physical test data sets conducted with the aluminium HC block. This proposed deceleration feature should be reusable, repeatable and sustainable. It is preferable to find a solution that could be industry friendly and tunable for different load cases.

The following are the design criterias listed by the company :

Deceleration: The new system or deceleration feature should withstand the high impact loads and decelerate the sled in a controlled manner, without bottoming out. The system should replicate the acceleration curve of a regular car crash.

Re-usability: The system must return to its initial condition for the next test to be conducted within a stipulated time frame. The number of test conducted is one per hour since it can take time to fit a new airbag for testing, to reset the sled and the HD. Hence, the new system should reset for the next test within one hour.

Tunability: The test setup is currently designed to test the PAB with a 50 percentile half dummy. The system should recreate the real life crash scenarios with different load cases, by varying the HD, mass and impact velocity. The combined mass of sled and HD could be varied from 78 - 95 Kg, and the impact velocity could be varied between 8 - 14 m/s.

Repeatability: A good test setup should produce similar results for similar load cases. The new system to be designed should not lose its capabilities over overtime or drop in its efficiency, leading to inconsistent results, making the results untrustworthy. The system should reproduce the same test results for same load cases to ensure the precision of the test setup.

Packaging space: The current test setup is confined to a space around the IP framework. There is a possibility to increase the length of the rail but currently the space above the anvil and the HC packaging space is restricted. The new system must fit compactly in the limited space available as shown in Figure 1.

With the proposed system of deceleration, a complete product assessment is to give a

conclusion, from building the CAE model to running simulations that can match the existing test result. An extended objective is to test the CAE model with different load cases, as it is feasible and more cost effective for an industry to conduct several simulations, than using a physical test setup.

1.3 Understanding the existing test setup

The existing test setup consists of components as shown in Figures 6 and 7.

Rail box: It houses the guide rails and serves as the foundation to the test setup. In the current design, the anvil is placed at the front end and have a buffer space that could be used to fit into the IP rig.

IP Rig: It holds the instrument panel and the airbag fixtures. It is intended to replicate the driver and passenger side of a commercial vehicle. Currently, the rail box is only on the passenger side of the rig to test PAB. The CAE model does not represent the exact IP test rig, but rather a template of a regular vehicle, as shown in Figure 7.

Anvil: It has a compartment in which the HC is placed and also acts as a hard stop if in case the HC fails to decelerate the sled .

Honeycomb: The HC pores are oriented longitudinally to the impact direction, resulting in increased longitudinal stiffness. The Young's modulus of the existing HC is 70 GPa. The HC CAE model can be seen in Figure 7.

Sled: It is the component that is accelerated into the HC at the required velocity and holds the HD. The sled allows the HD to replicate the motion of a unbelted human associated during a vehicle crash. The two A pillars, illustrated as black pillars in the Figure 6, contain a net that catches the HD during rebound.

Half dummy : A CAE model of the HD was built using a 50th percentile Humanetics Hybrid III model. The limbs and lower body were removed, leaving behind the torso and the head region that is sufficient to evaluate the PAB.

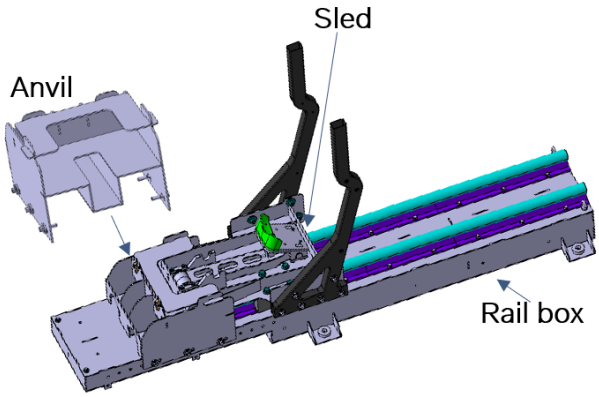

Figure 6: CAD model of the test setup

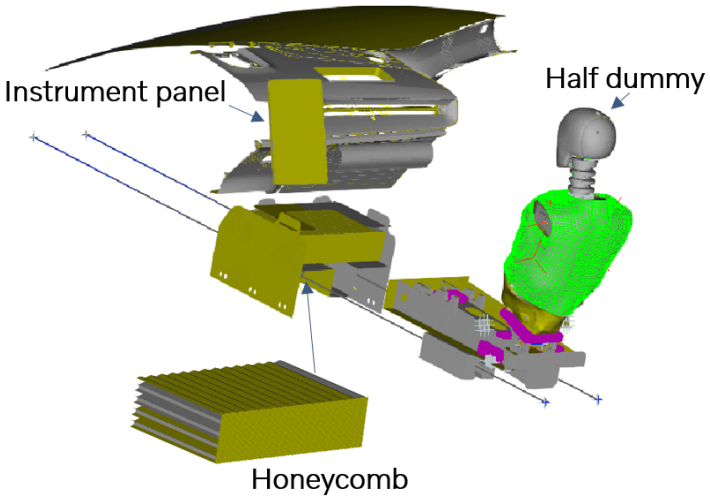

Figure 7: CAE model of the test setup

1.4 Scope

- For velocities greater than 12 m/s, the HC bottoms out and the data exhibits unusual behaviour. As a result, for velocities greater than 12 m/s, the CAE model cannot be correlated.
- The test setup with HC block is to replicate a real life frontal crash scenario. Recreating the existing test result with the damper as an alternate deceleration feature is two steps away from the reality of the frontal crash.
- There is limited space between the rails and instrument panel for designing the placement of a deceleration feature.
- The resources and knowledge in modelling the dynamics of damper in LS DYNA using finite element techniques are limited.

2 Theory

2.1 Selection of analysis type

The type of analysis to be carried out on a system can be classified based on the significance of inertial force ($m\ddot{x}$) , damping force ($c\dot{x}$) and the spring deformation force (kx) in the dynamic equation of motion (Eqn. 1) , where F_e is the time varying external force on the system.

$$m\ddot{x} + c\dot{x} + kx = F_e \tag{1}$$

Static analysis

Static analysis best suits for a system that is under investigation for a long time frame and the force is essentially constant throughout. The significance of inertial forces and damping forces can be neglected in this analysis, resembling human sitting on a seat.

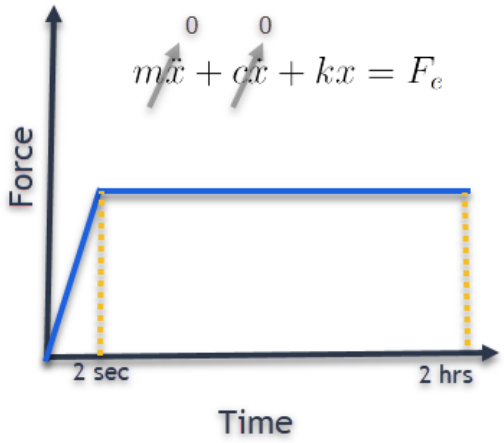

Figure 8: F vs T graph for static analysis

Steady state dynamic analysis

Steady state dynamic analysis implies a system that has a harmonic force in the specified time frame. The influence of inertial, damping and spring forces are quite significant in this type of analysis, resembling rotor in a motor.

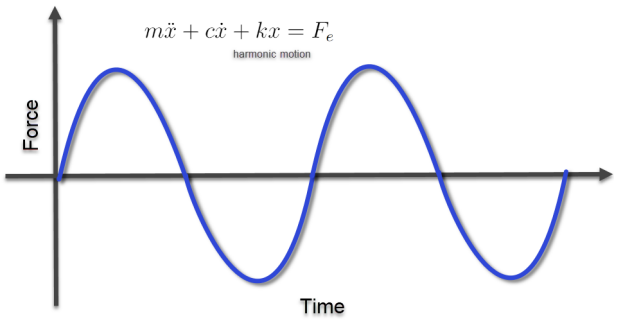

Figure 9: F vs T graph for steady state dynamic analysis

Modal analysis

A modal analysis implies a system that is disturbed and left to slowly adjust to its natural frequency, resembling a simple pendulum set into motion. The influence of the structural damping can be neglected in this analysis.

$$\omega_n = \sqrt{\frac{k}{m}} \qquad \omega_d = \omega_n\sqrt{1-\zeta^2}$$

Transient dynamic analysis

Transient dynamic analysis suits a system that is not harmonic in nature and occurs to due to sudden impact in a very small time frame. The time frame (T) for this analysis is usually in milliseconds and the inertial forces are significant in this analysis.

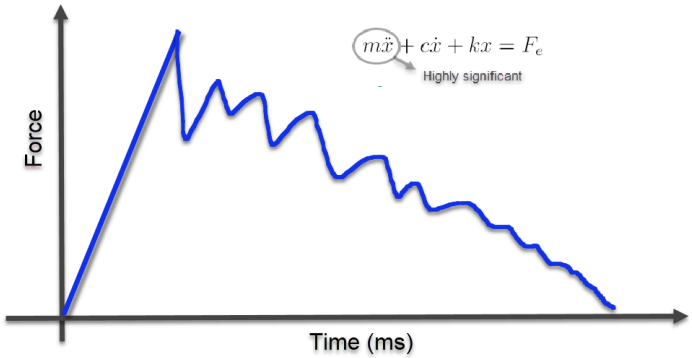

Figure 10: F vs T graph for transient dynamic analysis

The transient dynamics analysis is best suited for the given problem of decelerating the sled, as the time frame of the crash is occurs in 35-45 ms with high inertial forces.

2.2 Crashworthiness (physics of a vehicle crash)

When considering a scenario in which an occupant is traveling in a vehicle on regular roads. At time $T = 0^-$ (moment before the crash), the occupant and the vehicle travel at the same speed, i.e. relative velocity between the passenger and vehicle is zero ($V_{rel} = 0$). At time $T = 0^+$ (moment after the crash), the vehicle hits an obstacle and begins to slow down, whereas the occupant continues to travel at the same speed until obstructed by an instrument panel or a steering wheel. The front end of the vehicle is crushed and absorbs energy, slowing down the rest of the vehicle. The principle of crash can be obtained from Newtons laws [4] for Mass (M), Velocity (V), Force (F) and time (t)

$$\text{Change in momentum} = \text{impulse}$$
$$M * \Delta V = F * t \tag{2}$$

considering the moment to be equal for two different crash scenarios

$$F * t = \text{constant}$$
$$hence$$
$$F \propto \frac{1}{t}$$

This demonstrates that for a very short period of time, very large forces are involved, or in other words, a good vehicle should be able to absorb a large amount of force in a very short period of time. All safety features in automobiles, such as airbags, seat belts, and front ends, are designed to absorb crash forces using this principle.

Inspecting two crash scenarios[1] in which the front end of vehicle A is crushed to 0.3 m length and the front end of vehicle B is crushed to 0.6 m length. Vehicle B's stiffness is less than that of Vehicle A, so the crush is greater. The effect of mass is also crucial in the crush of the vehicles; the rigid barrier's mass is considered to be significantly greater than the mass of both Vehicle A and B. According to observations from both crash results, if the occupant in Vehicle A experiences around 40 g deceleration, the occupant in Vehicle B can experience around 20 g deceleration, because the time the force acts on the occupant in Vehicle B is doubled due to twice the crush distance.

[1] Assuming that the effect of frontal packaging space, geometry and mass of the vehicle A and B to be identical

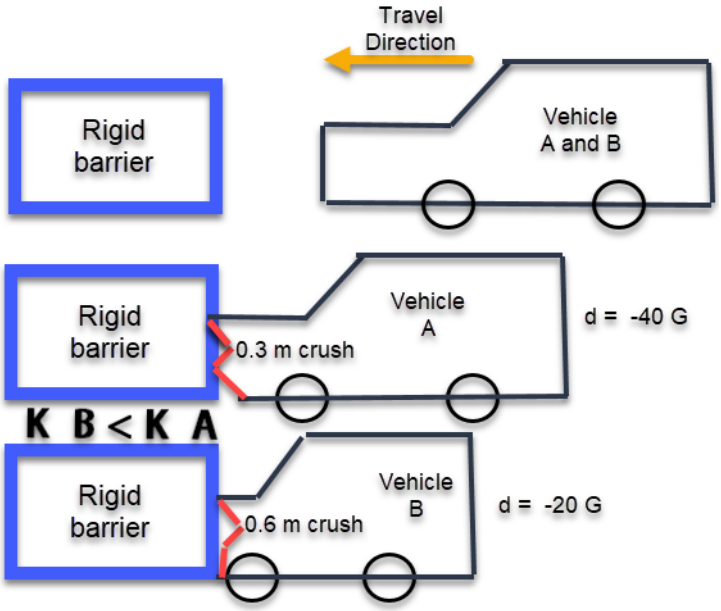

Figure 11: Crash worthiness example

In the automotive industry, crash worthiness refers to a vehicle's structural ability to plastically deform while still maintaining a sufficient survival space for its occupants in crashes with reasonable deceleration loads [5]. The aim of the test setup was to simulate the physics of a vehicle during a crash while also mimicking the kinematics of a human with a HD. The HC is crashworthy because it crushes while absorbing heavy sled impact loads. The HC resists load transfer to the other components of the test setup, thereby preventing the test setup from damages. These crashworthiness characteristics could be similar to the vehicle's front portions ability to absorb maximum impact loads, culminating in the loads not being transferred into the passenger cockpit. The proposed deceleration (energy absorption) system is meant to mimic the crashworthiness of the HC while also being reusable for multiple tests.

2.3 Alternate deceleration systems for the sled

To decelerate the sled, various deceleration systems that could potentially replace the HC were analysed. The deceleration system could either be a newly formed composite material block or a dynamic system. These deceleration systems should meet the design criteria [2]. The following are a some of the identified deceleration systems:

Arrestor gear using high tension cables: The sled could engage on to unidirectional cables that winds itself with a help of an arrester, causing the sled to

[2]Design criterias discussed in detail in Section 1.2

decelerate. Similar cables that are typically 2.5 to 3.2 cm in diameter[6] are used in decelerting military aircraft carriers.

Memory foam composite, Expanded Polypropelene and Nitinol composite: Memory foams and composites are widely used in the automotive safety as crash boxes, bumpers and side impact protection systems [7]. Poly urethene foams [8] of density 30 - 400 kg $/m^3$ are used in the industry as well for various purposes. Nitinol composite is a shape memory alloy that remembers its original shape and regains it upon unloading. The drawback is that it only has 8% strain recovery rate[9] [10].

Scissors lift X: Generally used to raise or lower a platform using hydraulics. A similar concept in horizontal direction, where the platform can be moved back to its original place in a controlled manner. The stack up and the movement of the support frame could be good replica to the HC's crush characteristics.

Springs with locking mechanism: The idea is to replace the HC block with springs of equivalent stiffness. Since, rebound is not preferred in the crash test rig, a locking mechanism is required to hold the spring.

Balloon mechanism: Conceptualised as a re-inflatable airbag with a larger surface area capable of absorbing energy. The medium of the balloon could be a fluid or foam pellets, with the filler element either escaping (open loop) or being reused (closed loop). The drawback is that there are inadequate resources to conduct in-depth fluid analysis on the filler element inside.

Dampers: The damper is effective in converting the kinetic energy of the impact object into heat and noise through friction. The test lab employs a wide range of dampers for a variety of purposes, proving to be industry-friendly in terms of installation and service.

2.4 Acceleration, velocity and displacement plots

The acceleration, velocity, and displacement plots aid in visualizing the crash dynamics, therefore understanding these plots is crucial. A crash system is depicted in Figure 12. A crash event can be divided into four time frames (A,B,C,D,E), as shown Figure 12.

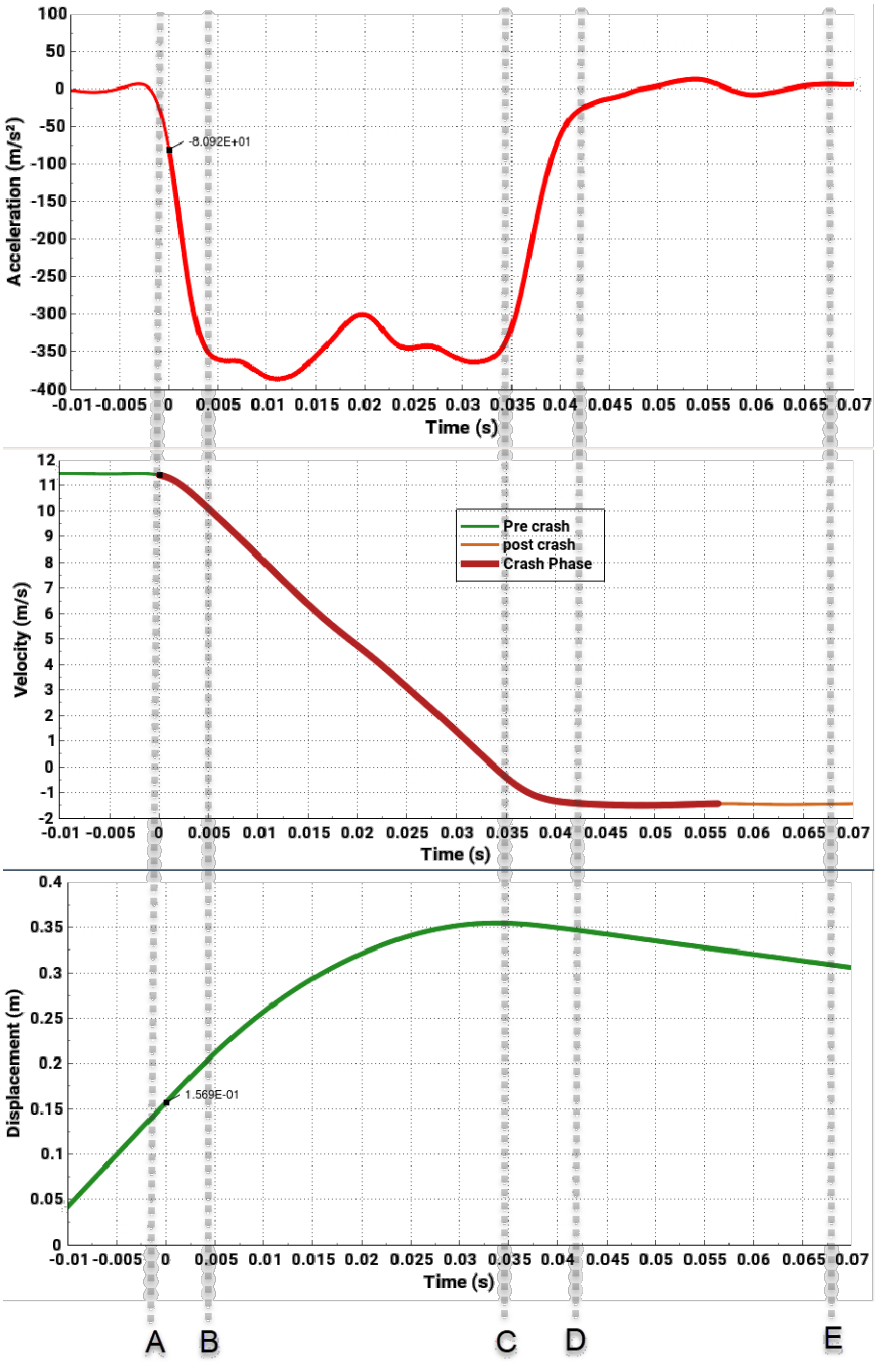

Figure 12: Bench marked test data acceleration, velocity and displacement plots

The crash propagates from point A, where there is a large peak in the acceleration plot (or the deceleration pulse), to point B. During the interval the velocity begins to drop as well.
Phase B-C is the energy absorption phase with the highest acceleration. In the acceleration plot, the curve plateaus in this phase. An unusual sudden peak in the plateau phase indicates that the system has bottomed out and is no longer able to absorb energy. Another interesting crash parameter is the ΔV, which can be estimated by subtracting the velocities from points A and D. This ΔV is critical for predicting the severity of the crash.
The system begins to approach rest at point C, where the acceleration approaches zero. The system begins to rebound from this stage on owing to its elastic nature. The difference between the displacements from points C and E is the rebound displacement.
The plots in Figure 12 are the plots obtained from the test setup using the HC. These plots are to be recreated with the new deceleration system.

2.5 Force, deformation and velocity characteristics

A complex crash scenario consisting of multiple elements can be reduced to a simple system as depicted in Figure 13, which consist of a single element mass, damper and a spring.

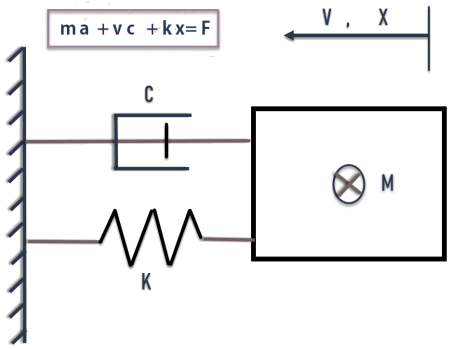

Figure 13: Schematic sketch of a crash system

The area under the force (F) vs. Displacement (D) curves represents the energy absorbed in the system during a crash event, which is critical in designing a deceleration system. The system begins with a negligible elastic response and the actual deformation recorded in the plastic response until it reaches the crush limit. The system then tends to unload, resulting in an elastic response with a rebound effect, as shown in Figure 14. It should also be noted that the slope obtained from the F vs. D curve is the system's stiffness (N/m).

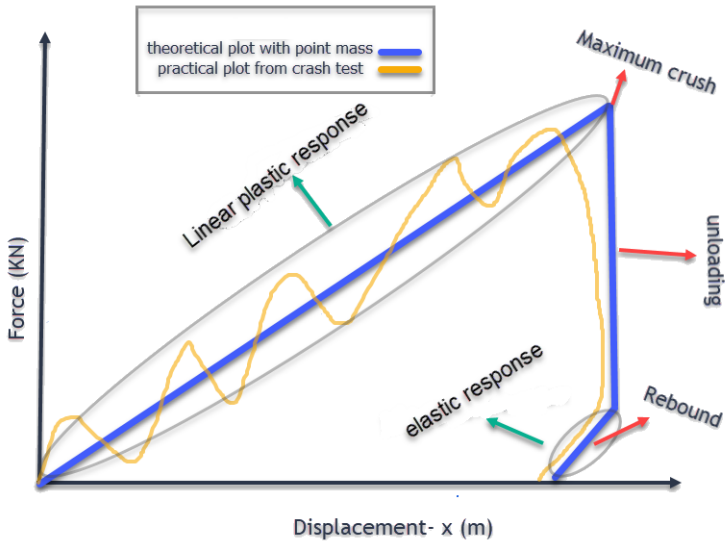

Figure 14: Force vs. Displacement curve

The force vs. velocity (V) plot is similar to the system's behaviour as mentioned in Figure 14. This plot is the main parameter required in modelling a damper. The area of F vs. V curve represents the amount of energy transferred per unit time, i.e. power (Watt) whereas the slope of the curve is system's damping coefficient (kN-s/m). The system's damping coefficient (DC) between the points A and B is calculated approximately as 4.16 kN-s/m as shown in Equation 3. The implementation procedure and the significance of the this F vs. V curve is explained in Section 3.4

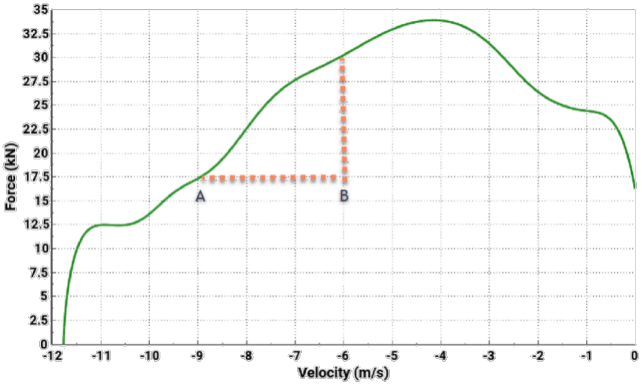

Figure 15: Force vs. Velocity curve

$$\begin{aligned} \text{Slope}_{A,B} &= \frac{y_2 - y_1}{x_2 - x_1} \\ &= \frac{30 - 17.5}{-6 - (-9)} \\ &= 4.16 \end{aligned} \tag{3}$$

2.6 Units in LS Dyna

When using the LS DYNA platform, consistent units must be prescribed. Figure 16 highlights the most appropriate set of units for mass (M), length (L), and time (T) utilized to understand the system throughout the thesis research. A crash incident occurs in less than a second, and the time required for an air bag to completely inflate is approximately 35-40 ms. As a result, it is more convenient to deal with ms for "T," and according to industry best practices, "L" was set in mm and "M" in kg.

MASS	LENGTH	TIME	FORCE	STRESS	ENERGY
kg	m	s	N	Pa	J
kg	cm	s	1.0e-02 N		
kg	cm	ms	1.0e+04 N		
kg	cm	us	1.0e+10 N		
kg	mm	ms	kN	GPa	kN-mm
g	cm	s	dyne	dyne/cm²	erg
g	cm	us	1.0e+07 N	Mbar	1.0e+07 Ncm
g	mm	s	1.0e-06 N	Pa	
g	mm	ms	N	MPa	N-mm
ton	mm	s	N	MPa	N-mm
lbf-s²/in	in	s	lbf	psi	lbf-in
slug	ft	s	lbf	psf	lbf-ft

Figure 16: Consistent units used in LS DYNA.[11]

2.7 Calculations

An internal test of was selected throughout the project. The average acceleration and damping coefficient in the system, can be determined by interpreting the sled as a element mass connected to a spring and a damper as shown in Figure 3. The parameters for calculations are as follows:

$$\text{Mass (m)} = 86.4\,kg \tag{4}$$

$$\text{Velocity (v)} = 11.82\,m/s \tag{5}$$

$$\begin{aligned}\text{Kinetic energy (K.E.)} &= \frac{1}{2} * mv^2 \\ &= \frac{1}{2} * 86.4 * 11.82^2 \\ &= 6035.58\,J\end{aligned} \tag{6, 7}$$

Since change in energy is work done

$$\text{K.E.} = \text{Workdone (W.D.)}$$
$$\text{W.D} = \text{Force (F)} * \text{deformation (d)}$$

Honey comb deformation(d) from test data is 203mm

$$\begin{aligned} \text{F} &= \frac{\text{W.D}}{\text{d}} \qquad (8) \\ &= \frac{6035.58}{0.203} \\ F &= 29731.89\ N \qquad (9) \end{aligned}$$

also,

$$\begin{aligned} \text{F} &= m * a \qquad (10) \\ \text{a} &= \frac{F}{m} \qquad (11) \\ &= \frac{29731.89}{86.4} \\ a &= 344.12\ m/s^2 \qquad (12) \end{aligned}$$

Considering the system with pure damping condition and no external force acting on the system. The structural dynamic Equation 1 can be simplified as

$$\begin{aligned} m\ddot{x} + c\dot{x} + 0 &= 0 \qquad (13) \\ 86.4 * (-344.12) + c * (11.82) &= 0 \\ c &= \frac{29731.89}{11.82} \\ c &= 2515.39\ Ns/m \end{aligned}$$

In Equation 13 the sign of acceleration is negative as the damping action causes the mass to decelerate.

3 Methodology

Figure 17 describes the work flow of the thesis. Once the problem was identified to decelerate the sled, data collection and analysis were crucial. From the many conducted tests, one good test result was chosen for benchmarking. Further, a survey was done on various alternate impact deceleration systems and dampers were chosen among them as the practical option that could satisfy all the design criteria. The selection process is explained in the Section 3.1. FE modelling of the simple systems and full scale system is explained in Section 3.2 - 3.6. The procurement, redesign, and testing of the designed deceleration system could not be completed within the 20-week time frame.

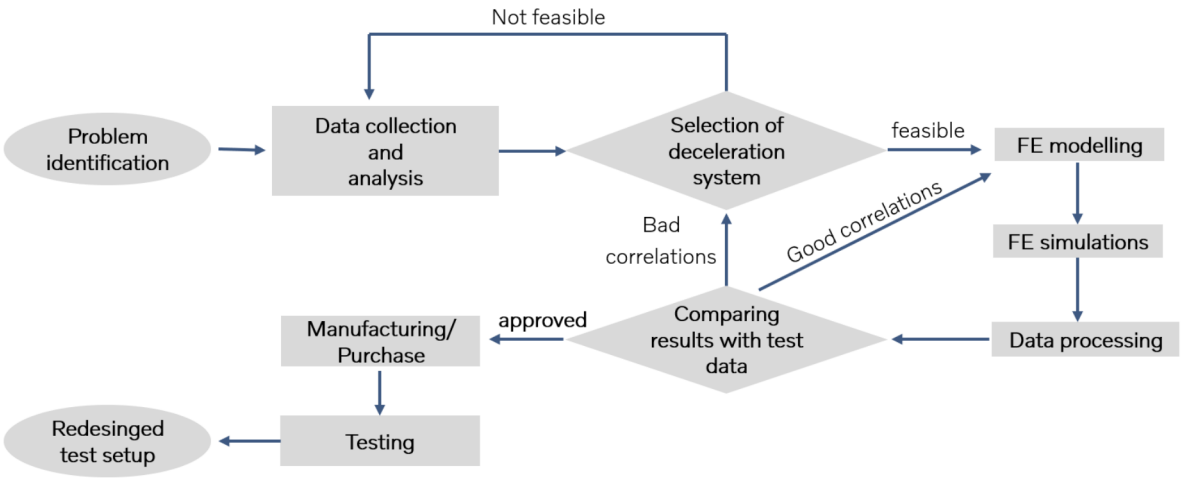

Figure 17: Flow chart of methodology

3.1 Selection of Damper system

Comparative studies were carried out on each design options to decelerate the sled, to find the best alternate to the HC. In industry, heavy equipment sleds are decelerated utilizing frictions brakes or magnetic resistance brakes. These features were not studied as modification on the rails and sled was restricted, due to design constraints.

A criteria-based decision-making matrix known as the Pugh matrix [12] is used to finalize on a potential solution for the given problem description in order to find an optimal solution among the various alternate deceleration systems. The Pugh matrix aids in prioritizing the criteria for developing a specific system. Section 1.2 discusses the five design criteria for replacing the honeycomb. Various design options were investigated in order to decelerate the sled while still replicating the

curves from the test results. Each design criteria is assigned a weight based on its priority.

Each design option can be marked with a "+1" if it is predicted to be more competent than the existing design with honeycomb, a "−1" if it is less competent, and a "0" if it is equal to the honeycomb's performance. Once each criteria for each design option has been scored, the total weighted score waas calculated, which aids in ranking the design option.

3.2 Building simplified FE models of the crash test rig

Modelling the damper system was the next stage in the thesis. This was done using the discrete element option in the LS DYNA platform. A general practise in the industry is to design a damper using a multi or rigid body analysis tool such as ADAMS, but the challenge is to be able to model the damper in the finite element analysis using LS DYNA, to have a common platform to integrate new designs into the existing CAE model.

To understand the physics behind the discrete element, the entire sled can be simplified into a plate or a point mass element. The influence of an airbag is neglected in the simplified model. Different simplified models were created to be able to replicate the sled decelerating as shown in Figure 18. A movable plate was made to replicate the damper's head, and an impactor plate was built to replicate the sled impacting the damper. The sled's boundary conditions such as the velocity and mass is assigned to the point mass, the movable plate and impactor plate respectively in these simplified models shown in Figure 18.

3.3 Variations in the simplified FE damper model

The energy to be absorbed by the damper is 6-6.6 kJ in a timeframe of 35-40 ms. Combinations of discrete element in series and parallel might be required to solve the problem as the energy is high and time period is very low. Different combinations of models with dampers and springs in series and parallel were created and tested.

As shown in Figure 19a, two dampers are connected in parallel to the movable plate. The drawback of this method is simultaneous contact of the sled with both the dampers would not be precise. Similarly, a FE model of a spring with low stiff-

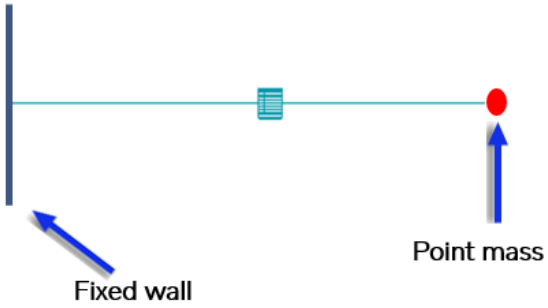

(a) Model with point mass

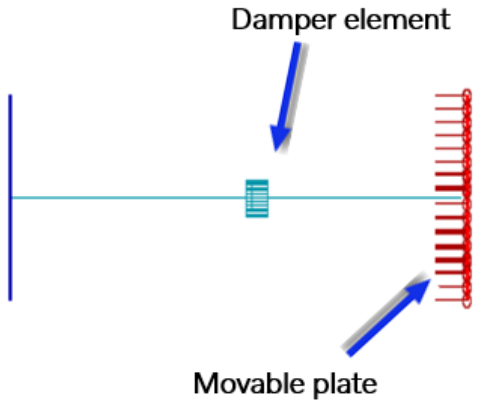

(b) Model with moving plate

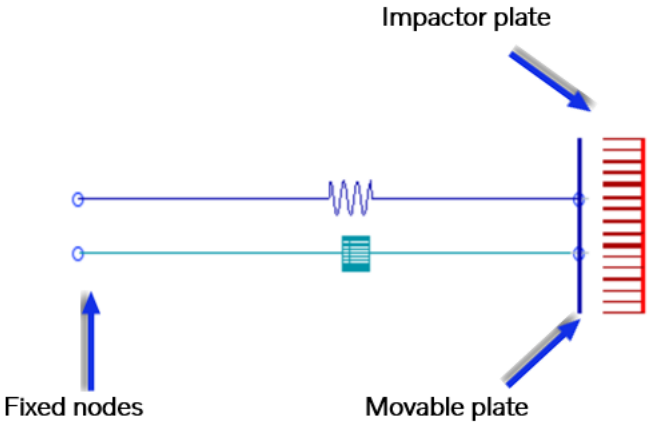

(c) Model with impactor plate

Figure 18: Simplified models to replicate the sled

ness is modelled in parallel to the damper, thus creating a model that represents a shock absorber, as shown in Figure 19b. This is to numerically achieve a small rebound displacement of the impacting mass after a crash.
Figure 19d shows two dampers connected in series. The motive of dampers in series connection is to achieve variable DC at different stages of the test. It is built by joining both the discrete elements by a node.

Though it is practically difficult to engage the spring later to the ideal damper, a model variation b was built as shown in Figure19c, to understand the influence on how a spring and a damper work together.

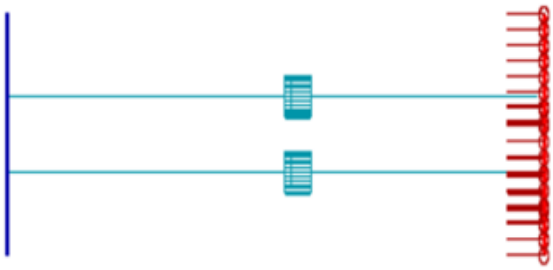

(a) Parallel connection

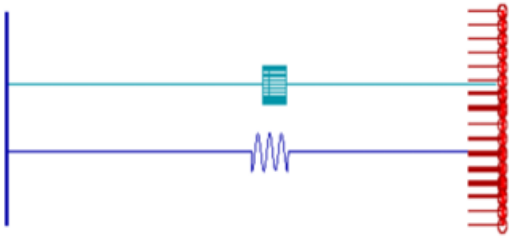

(b) Spring and damper effect together

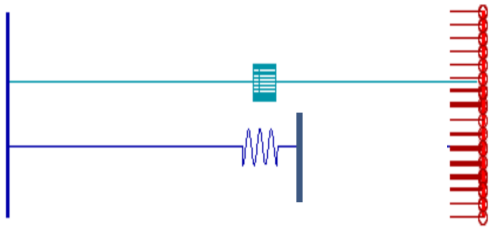

(c) Spring effect later to damper

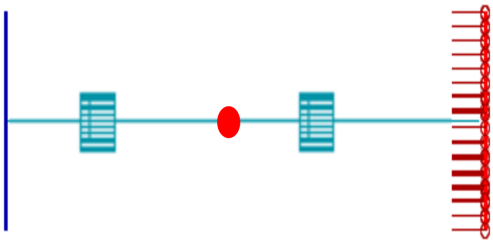

(d) Series connection

Figure 19: Variations in simple model

3.4 Linear and non linear viscous damper parameter study

To understand the response of a linear viscous damper and a non linear viscous damper for our system under consideration, simple analyses were made to compare the velocity curve variations with accordance to the change in DCs. The force vs. velocity input curves to the discrete element are crucial in understanding the response of the discrete element. The mean-squared error (MSE) method was used to calculate the deviations in the output velocity plots for each case studied.

3.4.1 Linear viscous damper

The input parameter for material damper linear viscous (MAT S02) in LS DYNA is the DC (kN-ms/mm), which will be constant throughout the range of velocity. The keycard (*MAT_DAMPER_VISCOUS) used from LS DYNA Manual Volume 2 [13] shown in Figure 21. Linear viscous damper means that the relationship between the force vs velocity is linear as shown in Figure 20. The dynamics of a linear damper were studied by increasing the DCs by 50% in intervals, beginning with 2 kN ms/mm (2000 Ns/m).

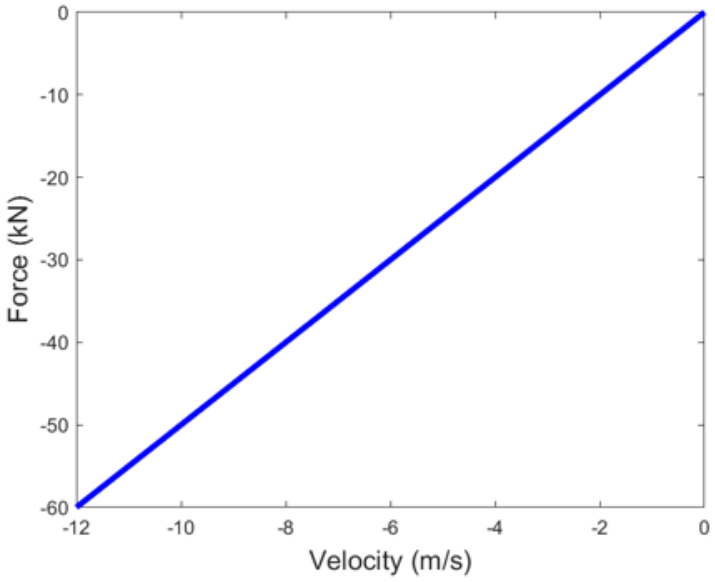

Figure 20: F vs. V for a linear viscous damper

***MAT_DAMPER_VISCOUS**

This is Material Type 2 for discrete elements (*ELEMENT_DISCRETE). This material provides a linear translational or rotational damper located between two nodes. Only one degree of freedom is then connected.

Card 1	1	2	3	4	5	6	7	8
Variable	MID	DC						
Type	A8	F						

VARIABLE	DESCRIPTION
MID	Material identification. A unique number or label not exceeding 8 characters must be specified.
DC	Damping constant (force/displacement rate) or (moment/rotation rate)

Figure 21: LS DYNA linear viscous damper material card

3.4.2 Nonlinear viscous damper

A non linear damper aids in variable DCs. This helps in obtaining tunable stiffness in the damper model at different stages. The *MAT_DAMPER_NONLINEAR_VISCOUS keycard from LS DYNA Manual Volumne 2 [13] is used as shown in Figure 22. The variable DC's are tabulated in Table 1. The DC1 is defined from 12 m/s to 4 m/s velocity and DC2 is defined from 4 m/s to 0 m/s. The piece-wise linear load curves for the non linear viscous damper are defined in ANSA as shown in the Figure 23. Different combinations of DCs are chosen to understand the dynamics of a non linear viscous damper.

Case	DC1	DC2
1	2	9
2	2	6
3	9	2
4	9	5

Table 1: DC values chosen for non linear viscous damper parameter study

***MAT_DAMPER_NONLINEAR_VISCOUS**

This is Material Type 5 for discrete elements (*ELEMENT_DISCRETE). This material provides a viscous translational damper with an arbitrary force as a function of velocity dependency or a rotational damper with an arbitrary moment as a function of rotational velocity dependency. With the damper located between two nodes, only one degree of freedom is connected.

Card 1	1	2	3	4	5	6	7	8
Variable	MID	LCDR						
Type	A8	I						

VARIABLE	DESCRIPTION
MID	Material identification. A unique number or label not exceeding 8 characters must be specified.
LCDR	Load curve ID defining force as a function of rate-of-displacement relationship or a moment as a function of rate-of-rotation relationship. The load curve *must* define the response in the negative and positive quadrants and pass through point (0,0).

Figure 22: LS DYNA non linear viscous damper material card

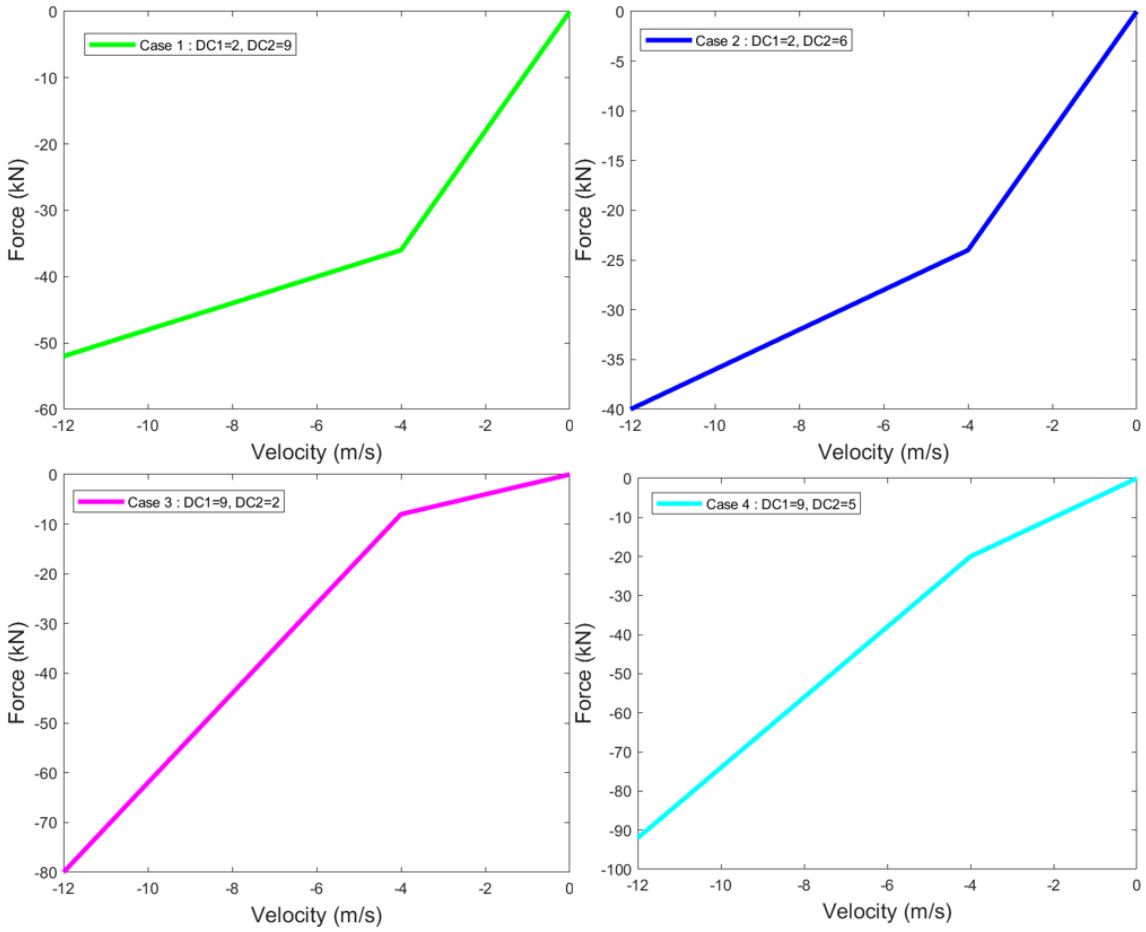

Figure 23: Load curves used for nonlinear viscous damper parameter study

3.5 Finalised simple FE model

Simplifying the problem of decelerating the sled to a mass of 87 kg travelling at a velocity of 12 m/s, decelerated by a damper (or shock absorber in this case) placed at one end within a stroke length of 350 mm.

Considering the simplified approach, a simple FE model of the system was created to understand the basic dynamics of the system. A pair of nodes were created at a distance of 350 mm from one and another in x-direction. One of these nodes was placed on the origin and is fixed in all directions, referred to as the "fixed node end". The other node has only one degree of freedom, i.e. translation in x direction only and is referred to as the "moving plate end". By using the discrete element option in LS DYNA, the two nodes were picked to create a discrete element between the two selected nodes. A non linear viscous damper material property has to be assigned to this discrete element to create a damper element. Similarly two more nodes were created to build the discrete element for the spring. The spring and the damper element are now parallel to each other in y-direction as shown in figure 24.

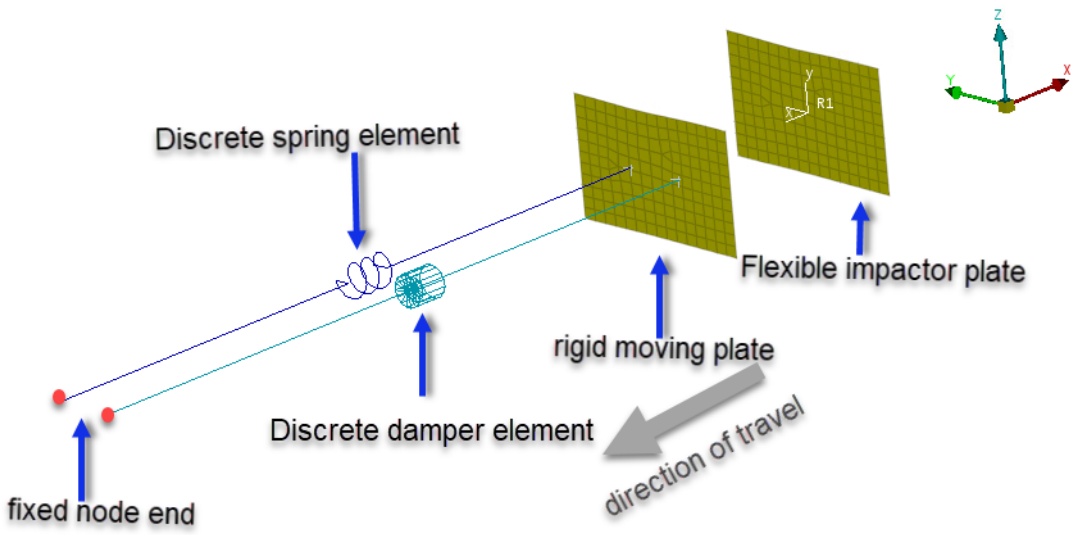

Figure 24: Selected simple FE model representing the test setup

Two plates with similar dimensions are modelled with 5 mm thick shell elements. One of the plates is referred to as "movable plate" and the other one as the "impactor". Maintaining a distance of 5 mm between the two plates will result in contact between the two plates at the time of impact. The movable plate is 350 mm from the origin in x-direction. The "moving plate end" nodes are constrained

to the movable plate by using the extra node command in LS DYNA(*CONSTRAINED_EXTRA_NODE)[3]. This command defines certain nodes as part of the rigid body.

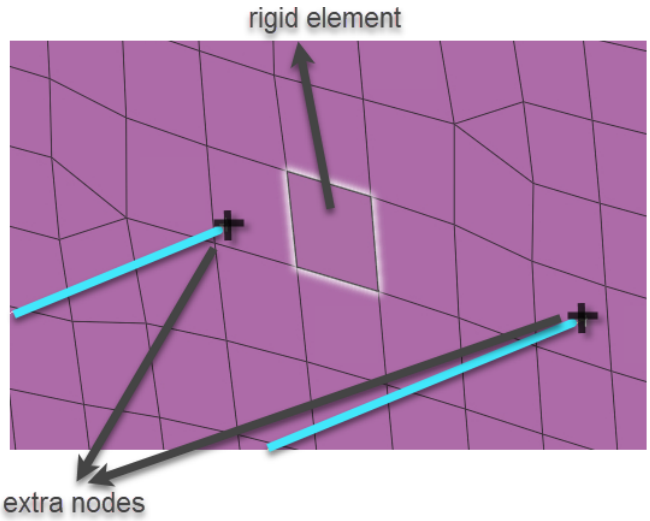

Figure 25: Assigning extra node to rigid element

3.6 Materials and properties for the simple FE model

As the impactor plate resembles the sled onto which the human body dummy is fixed, it's mass must be 87 kg. This can be done by either adding a point mass of difference in weight to a node on the shell plate or increase the density of the plate.

A good method to input the mass in ANSA is to alter the density (ρ) of the part rather than its directly using the element mass keycard. The thickness (b) is assigned as 5 mm in the part ID, suitable length (l) and height (h) of the damper plates were chosen to be 95 and 58.5 mm respectively. The input mass (m) of the entire sled and dummy is 87 Kg.

$$\begin{aligned} \rho &= \frac{mass}{volume} \\ &= \frac{87}{l \times b \times h} \\ &= \frac{87}{27787.5} \end{aligned} \tag{14}$$

$$\rho = 0.00314\ Kg/mm^3 \tag{15}$$

The material assigned to the movable plate is a steel rigid body (MAT 20) with

[3]command used on line 26 of A.1

x-translational as the only degree of freedom, whereas the material for the impactor plate is linear piecewise plasticity steel (MAT 24) with similar constraints. Although the behaviour of both the plates are same, i.e rigid, it is necessary to have at least some elastic elements in the model for LS DYNA to be able to compute the time step. The contact defined between the two plates is 'automatic surface to surface contact' with the movable plate as the master contact and the impactor plate as the slave contact. The coefficient of static friction and dynamic friction does not play a huge factor in our problem as the lateral movement between the two plates are negligible. Therefore, both friction values can range anywhere between 0.1-0.7 [14] for a steel on steel contact. The initial velocity of 12 m/s is assigned to the impactor plate in the negative x-direction.
The material assigned to the damper element is a non-linear viscous damper (MAT S05). It is a translational damper with a load curve defined of force as a function of rate of displacement as its input. Similarly the material assigned to the spring is a spring elastic (MAT S01) with stiffness (kN/mm) as the input.

3.7 Full scale FE model of the crash test rig with damper

A finite element CAE model of the crash test rig already existed with HC as the deceleration feature. This HC block and the holder anvil had to be replaced with a damper, spring and a movable plate as shown in the figure 26. The movable plate is exactly positioned where the front face of the HC is positioned at. The contacts are redefined between the sled carrying the HD (slave contact) and the movable plate (master contact) with same friction coefficients.

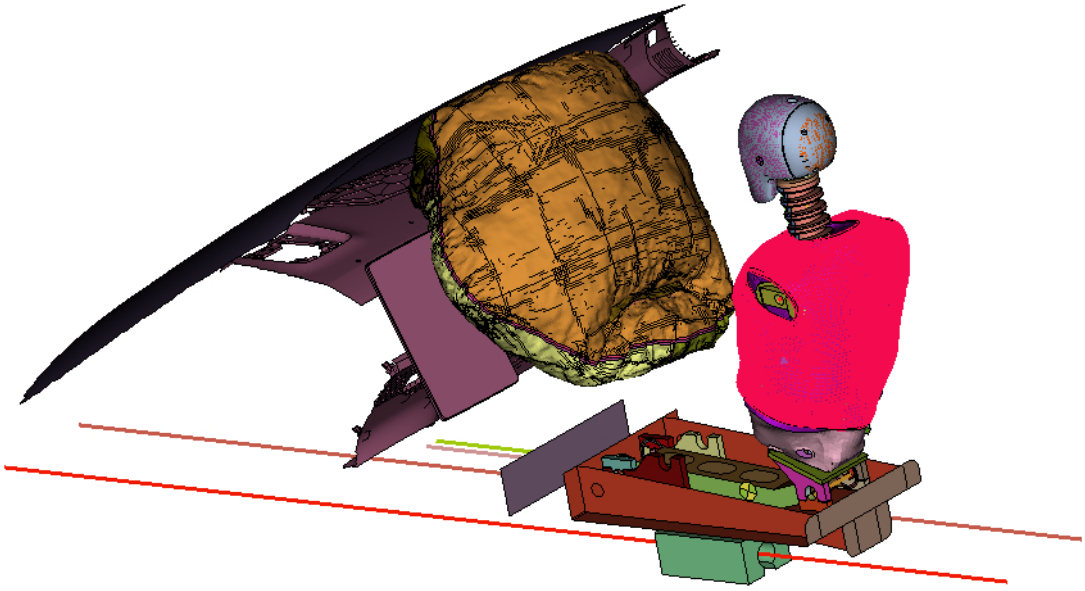

Figure 26: Full scale CAE model with damper

The initial velocity is assigned to the sled and the dummy in this full scale model. Although the given load case is 12 m/s, the velocity generated in the model is slightly lesser to 11.5 m/s. This is because in the physical testing, the velocity of the sled at the time of impact with the HC is 11.5 m/s due to friction and other resistances.

The piece wise linear load curve for a non linear viscous damper as in Figure 27 was used in the full scale CAE model with damper, along with the DC value of 0.09 kN/mm.

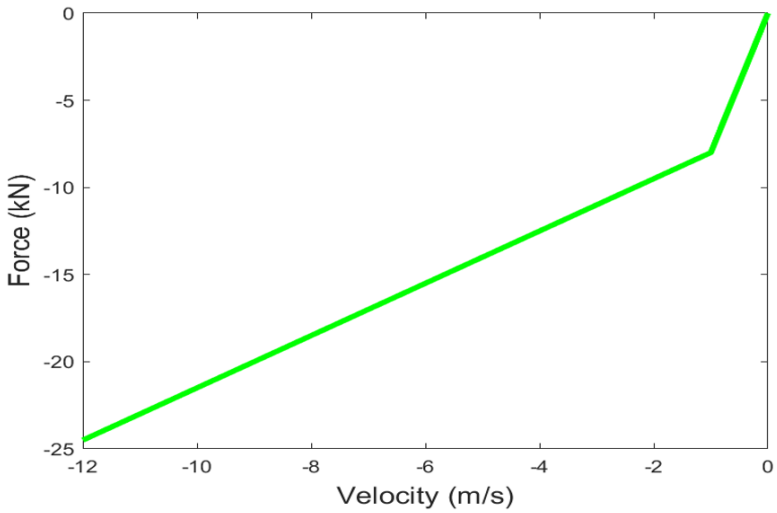

Figure 27: Load curve used for non linear viscous damper in full scale CAE model

4 Results

4.1 Design selection

Figure 28 depicts the Pugh matrix used to finalize the selection of the deceleration system. It can be noticed that the damper has the highest weighted score of 8 and is the appropriate system that can be a good replacement for the existing honeycomb. A damper system is also simple and cost effective for the company, as it can be installed into the existing test setup with minimal changes. The anvil must be redesigned to accommodate the damper, and the length of the rail box can be increased if necessary. The vertical packaging space is limited for other design options due to the IP rig.

Pugh Matrix

		Existing Design	Design Options								
Criterias	Weight	Honey Comb	High tension wires	Memory Foam Composite	Damper	Scissors Lift X	Nitinol Composite	Springs with locking mechanism	Rack, pinion and ratchet	Balloon mechanism	EPP (Expanded polypropelene) 5130
Deceleration	1	0	-1	-1	0	-1	0	1	-1	-1	-1
Repeatability	3	0	1	1	1	1	1	-1	1	1	1
Re useability	3	0	1	1	1	-1	-1	1	0	1	-1
Tunability	2	0	1	-1	1	-1	0	-1	-1	0	1
Packaging space	2	0	-1	0	0	-1	-1	-1	-1	-1	0
Total +1's			8	6	8	3	3	4	3	6	5
Total 0's			0	2	3	0	3	0	3	2	2
Total -1's			3	3	0	8	5	7	5	3	4
Weighted score			5	3	8	-5	-2	-3	-2	3	1
Rank			2	3	1	7	5	6	5	3	4

Figure 28: Pugh matix used for selecting alternate deceleration option

The damper can decelerate the sled in a controlled manner by meeting the design criteria. The damper can be fitted in the test rig with a new anvil design, demonstrating its cost effectiveness in comparison to other design options. Due to which, other design choices were not explored further.

4.2 Simplified FE models

The plot for the velocities in each of the simplified models are shown in Figure 29. It is noticed that running simple FE models with high computation power, the difference in simulation time is negligible. The results are similar for all three models. The result obtained from the FE model with impactor plate needs to be filtered (CFC 60) as there is continuous interaction and vibration between the movable and impactor plate.

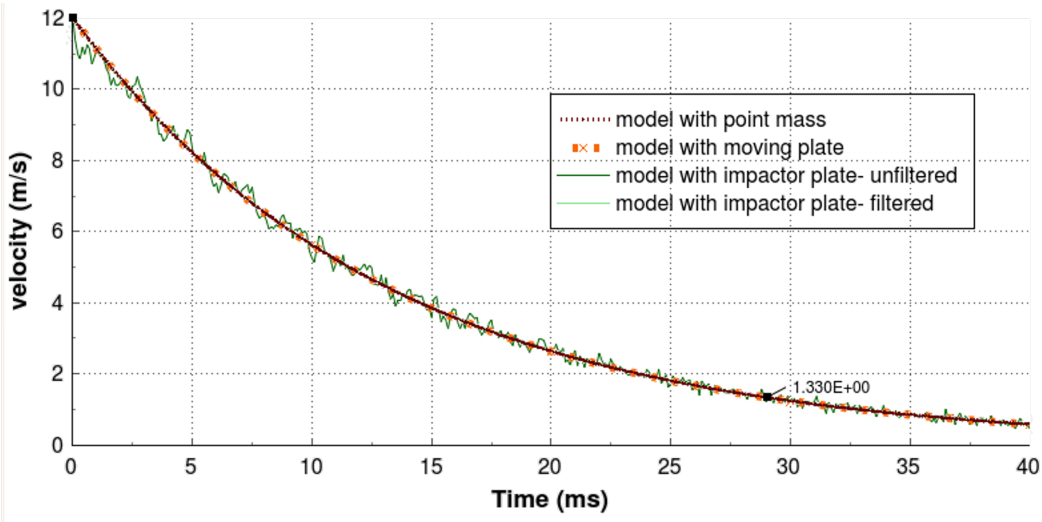

Figure 29: Velocity comparisons between simple FE models

Since there is negligible difference in computation time and result, the model with impactor plate was chosen to be the simple FE model as it is a more realistic representation sled contacting the damper head.

4.3 Variations in simple models

From Figure 30, it is noticed that connecting two dampers in parallel is similar to connecting one damper with equivalent DC. The sum of the DC's of the two parallel dampers is the equivalent DC. If the DC required is too high for a single damper, it can be solved by adding two equal but lower DC dampers in parallel. It can also be noticed that the final velocity of the impactor decelerated by dampers alone is 0 m/s. There is no rebound of the impactor plate in this case. This is solved by the shock absorber model. The damper absorbs most of the energy and the spring dissipates some amount of energy. This helps us to replicate the light rebound of the sled after the crash.

A working model of two dampers in series is not achieved as the series connection is built by joining both the discrete elements by a node. With only x translational dof, the second damper alone is actuated, whereas fixing the node in all directions leads to actuation of the first damper only. A different approach is taken to achieve this variable DC with a non-linear viscous damper.

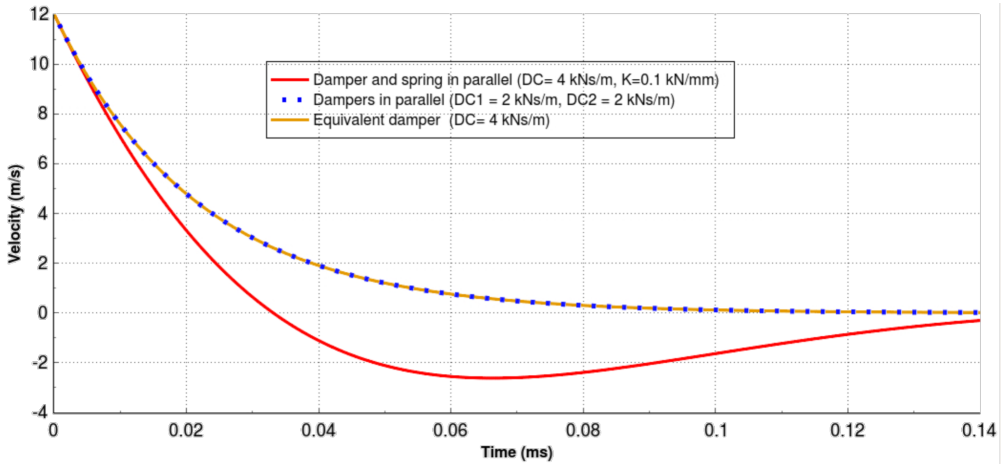

Figure 30: Velocity comparisons with variations in simple FE model

An example input for variations b and c were built with $DC = 4$ (kN ms/mm), and spring stiffness of 0.175 (kN/mm). From Figure 31 it could be observed that, though having a bare minimal spring stiffness, there is a huge rebound in the system in variation c of the simplified model. Hence this effect should be taken into consideration when building a model for the shock absorber, where the effect of a spring and damper act together from the time of impact.

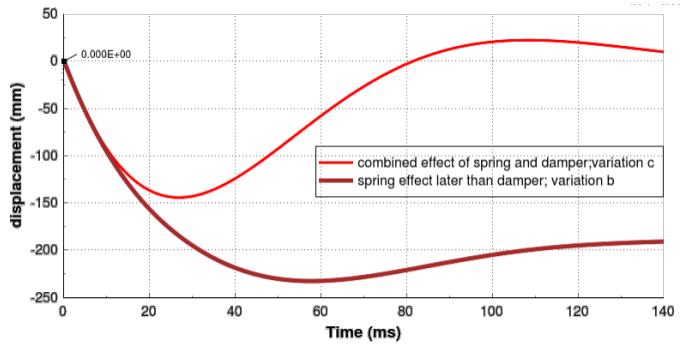

(a) Displacement comparison

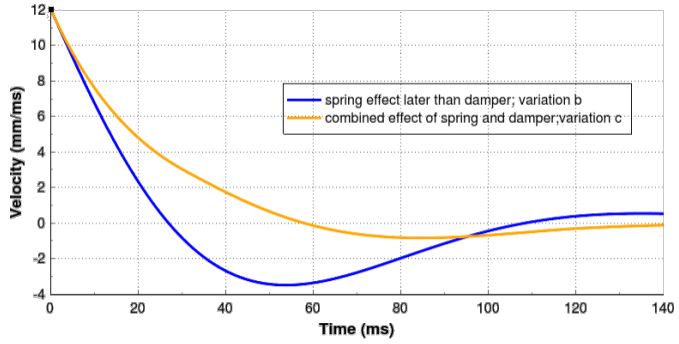

(b) Velocity comparison

Figure 31: Comparison between variations models b and c in simple model

4.4 Parameter study on damper element

4.4.1 Linear viscous damper

Figure 32 shows the change in the velocity of the impactor plate due to the damper with various DC values. It is noticed that as the DC is increased, the slope of the velocity plot (acceleration) is higher and the time taken for the impactor to attain complete rest is higher. Although, this could be solved with much higher DC, the required controlled deceleration is not achieved.

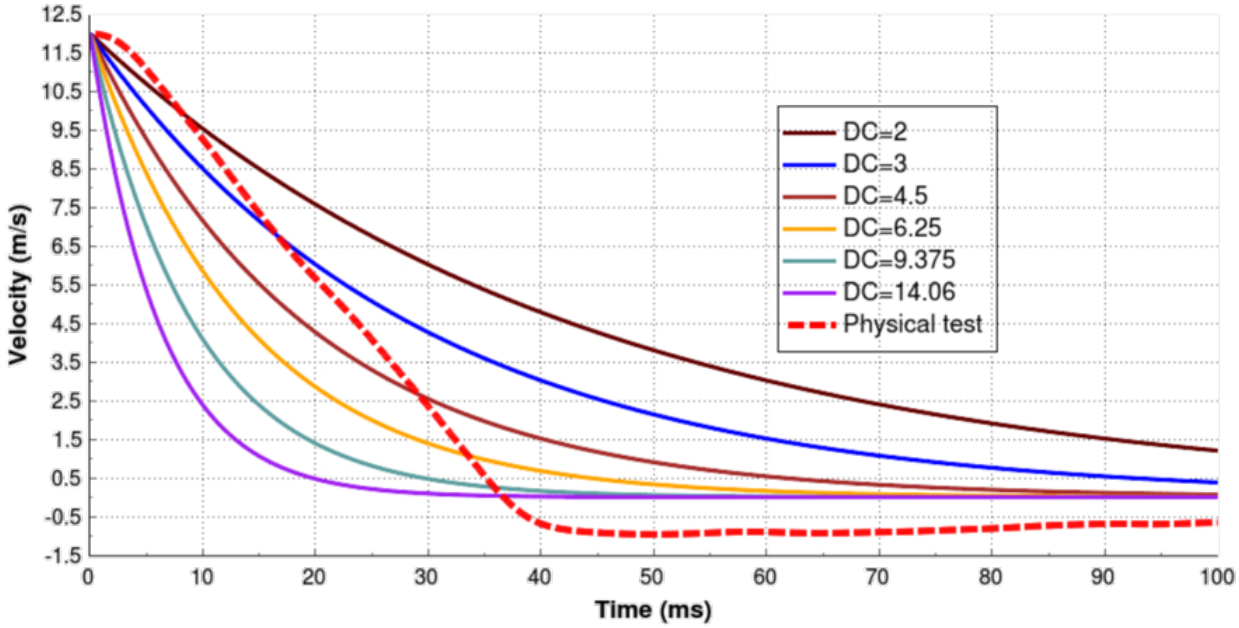

Figure 32: Linear viscous damper behaviour

4.4.2 Non linear viscous damper

The given input of force vs. velocity curves from Figure 23 results in obtaining the velocity plots as shown in Figure 33. Similar to linear behaviours the slope of velocity plot increases with the increase in DC. Case 3 and Case 4 have the same DC1 but different DC2. In both of these cases, the DC1 is higher than DC2. It can be noticed that the velocity plot of both the cases follow almost of a similar path upto 4 m/s. Case 3 deviates away, taking a longer time frame to come to rest due to lower DC2 compared to Case 4. As DC2 is lesser than DC1, the influence of DC2 before the velocity 4 m/s is less significant.

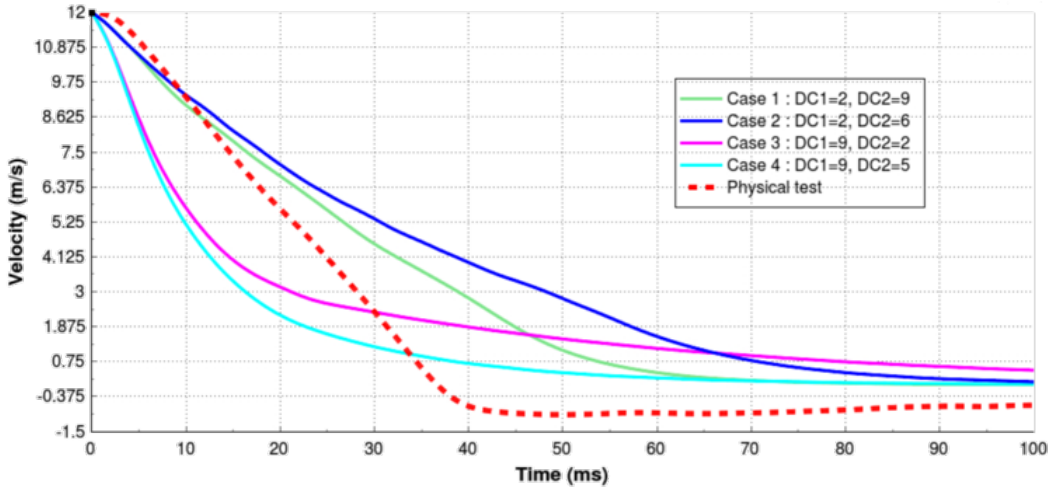

Figure 33: Non linear viscous damper behaviour

Similarly, case 1 and 2 also have same DC1 but different DC2, and DC1 is lower than DC2. The velocity plot for these cases also follow the similar path upto 4 m/s and Case 2 deviates away from Case 1. As the DC2 is much higher than DC1 in both of these cases, the influence of DC2 is quite significant before the velocity 4 m/s.

The more number of slopes (data) given in the input can help in refining the behaviour of the damper accordingly.

4.5 Comparing physical test and simple FE model

Figure 34 and Figure 35 shows the impactor's velocity and acceleration respectively.

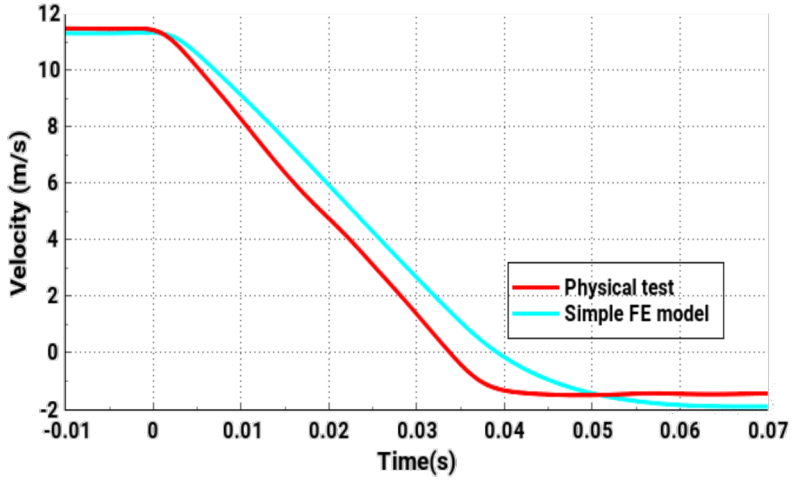

Figure 34: Velocity comparison between physical test and simple FE model

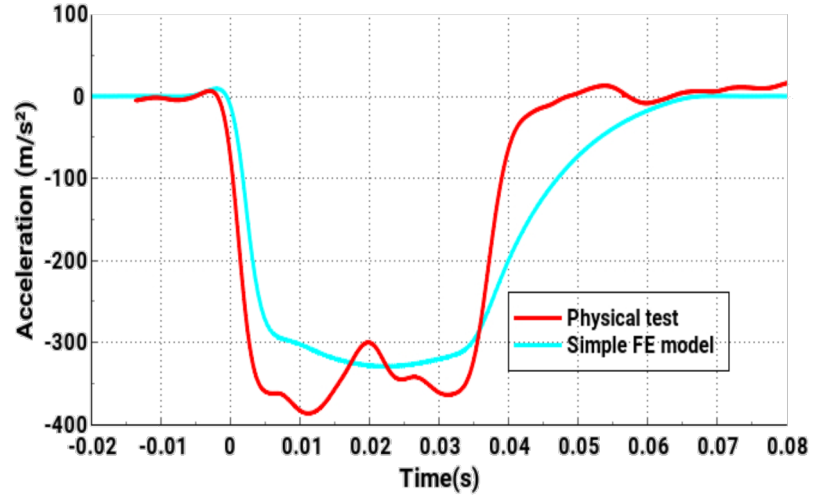

Figure 35: Acceleration comparison between physical test and simple FE model

It can be noticed that the simulation result is closer to the test data. The iterations with the simple model are stopped here with a MSE 1.2 m/s. The airbags and HD will have a considerable effect to the impactor plate's deceleration. This simple model with same damper and spring properties are next implemented into the full scale CAE model of the crash test rig.

4.6 Comparing physical test and full scale FE model with damper

The velocity and the acceleration plots of the sled carrying HD is shown in Figure 36 and Figure 37 respectively.

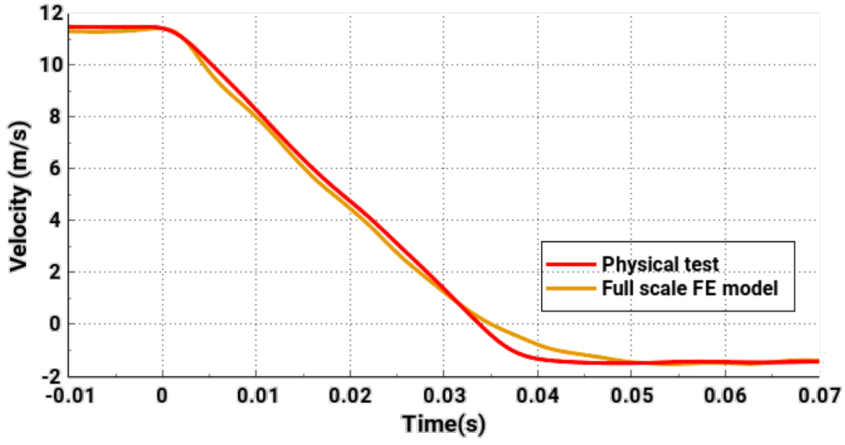

Figure 36: Velocity comparison between physical test and full scale FE model

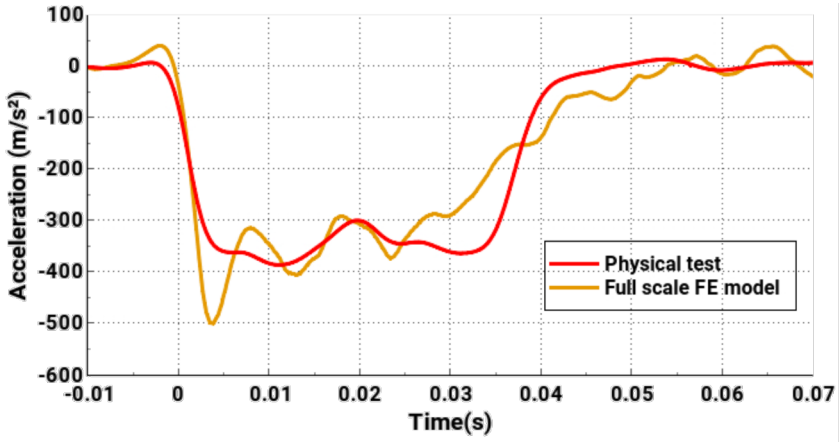

Figure 37: Acceleration comparison between physical test and full scale FE model

It can be seen that the full scale crash test rig CAE model is matching the test data from the time of impact to the -2 m/s. The mean squared error (MSE) between the two curves is 0.115 m/s. However, the rebound phase is not of much importance as the component testing is concluded when the sled reaches 0 m/s. The mean squared error (MSE) between the two curves from the time of impact to 0 m/s velocity is 0.0871 m/s. The force vs. displacement and the energy absorbed are shown in Figure 38a and Figure 38.

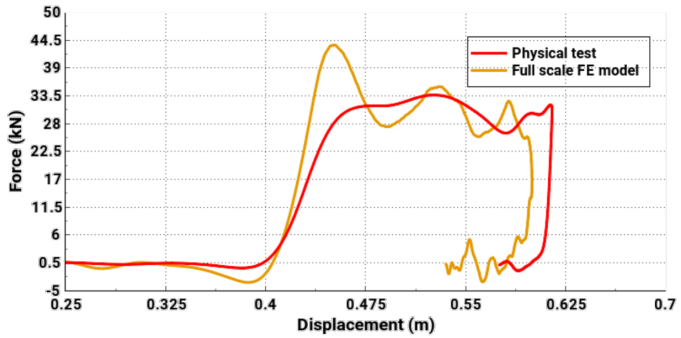

(a) F vs. D comparison

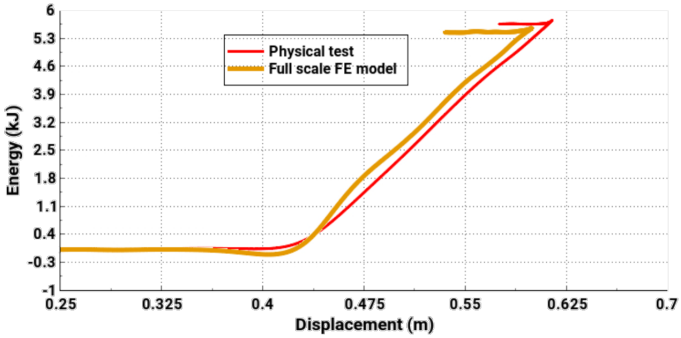

(b) Energy comparison

Figure 38: Force and energy comparison between physical test and full scale FE model

4.7 HIC Value comparisons

To verify that the damper system should not negatively influence effect the head injury criterion (HIC) values of the HD. The calculated HIC 15 values were compared between the physical test and the full scale CAE model with the damper in Figure 39.

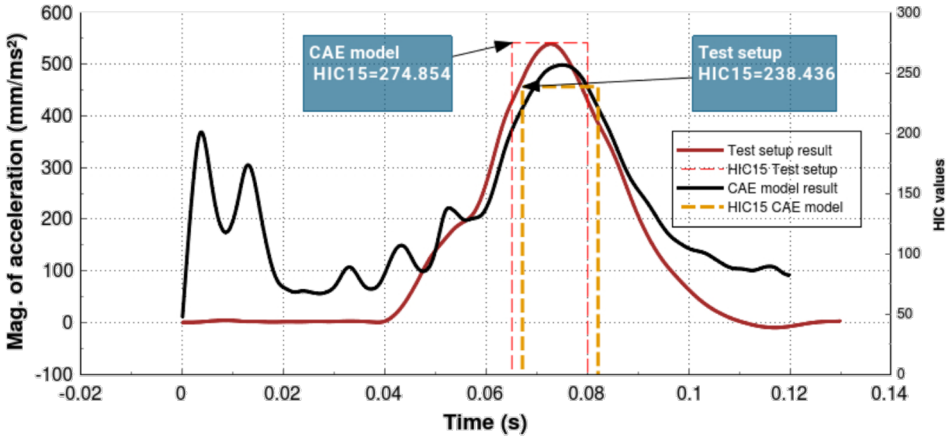

Figure 39: HIC comparisons between physical test and full scale CAE model with damper

The HIC 15 values calculated from the head accelerations of the HD were judged using Abbreviated Injury Scale (AIS) from Figure 40 [15]. For both the HIC 15 values from physical test data and full scale CAE model data obtained the AIS 1, 2, and 3 the injury probabilities lie in the same range.This proves that a damper system designed to decelerate the sled will not negatively impact the injury criteria on the dummy.

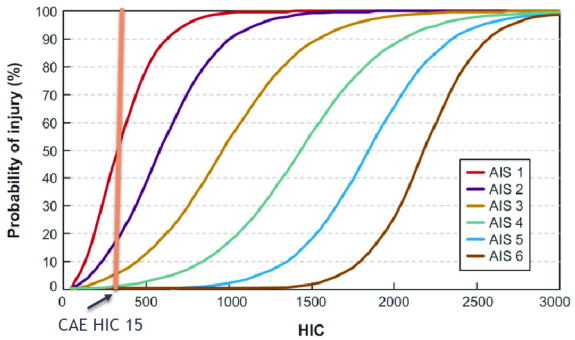

Figure 40: AIS injury criteria

5 Discussion

The objective of this thesis work was to check for a possibility to find an alternate to the HC in the test setup. This alternate method should make the test setup more robust and the results more repeatable for the same load case. Acceptable alternatives to the HC are discussed, as well as how a CAE model for the alternate feature was created. This section also highlights observations that are critical if the CAE model is to be used in the future.

5.1 Selection of an alternate to the HC

Various design options were evaluated that could be a suitable replacement for the HC by satisfying the given design criterias. After collecting data and brainstorming, the design options proposed were either a material or a dynamic system. An additional design restriction is that no modifications could be made on the rails but the rail box length could be increased. A comparative study using a Pugh matrix was used to find the best suitable deceleration feature out of the proposed design options. Each design criteria was weighted based on its priority and each design option was judged with a 0, +1 or a -1,were 0 denoting the performance equal to the HC and a positive or a negative performance was denoted with a +1 and -1 respectively. With the weighted scores, a damper could be the best suitable option to replace the HC. Also, various industrial dampers are already used in the industry, which is feasible for installation and maintenance.

5.2 Simple FE model with the damper

A simple model was built by simplifying the problem to only decelerating the sled without the influence of the airbags or the dummy. Multiple simplified CAE models were analysed to choose the right simple FE model set up. A spring and a damper, connected in parallel to a movable plate, was the most suitable simplified FE model that can replicate the entire crash test system.

5.3 Parameter studies on the damper element

Parameter studies were explicitly conducted on linear and non-linear viscous damper elements. This parameter study was performed to understand the damper element behaviour in LS DYNA. The calculated average damping coefficient(DC) result obtained for the damper was 2.5 kNms/mm. This DC was first tried with a linear

viscous damping material. The time taken for the impactor to come to rest was more than 100 ms. The analytical solution was considered to be an approximation and the result obtained does not decelerate the sled as required. Starting from a DC value of 2kNms/mm, the DC values were increased with 50 % at each step until 14.06 kNms/mm. The results from the parameter study on the linear viscous damper element could not achieve the controlled deceleration and a variable DC was required to achieve the desired controlled deceleration of the sled. This was analysed by conducting a parameter study with the non-linear viscous damping material.

Along with attaining a good knowledge to tune the damper, certain flaws and limitations of the non linear viscous damper material were found. The input load curve for the non-linear viscous damper is a piece-wise linear. The input load curve to the damper element is sensitive in the method it is defined. The damper load curve in the include script file must be defined in descending order of velocity. A non-linear viscous damper's final DC cannot be negative. In the described circumstances, the damper element exhibits abnormal results.

5.4 Implementing the damper element in full scale CAE model

By understanding the behaviour of the non-linear viscous damper from the parameter study conducted, multiple iterations were performed on the simple model that could decelerate the sled to resemble the bench marked physical test. The piece-wise linear load curve shown in Figure 27 was the input for the damper and the spring stiffness chosen was 0.009 kN/mm. The full scale CAE model with the damper takes 6 hours approximately to solve with 120 CPU's. Tuning the simplified FE model (dampers and spring elements in parallel) to attain the sled deceleration closer to bench marking data was advantageous. The mean squared error(MSE) was calculated to quantify the difference between the velocity plot from the physical test and the simplified FE model with the damper. A good approximation of correlation with the simplified FE model to the physical test data is when the MSE is +1.2 m/s. With this approximation the damper can be implemented into the full scale FE model. The waiting time can be reduced by achieving close computational solutions with the simple model. Good comparisons can be observed when comparing the physical test data and the full scale FE model with the damper. The difference in the results between the simple model and the full scale FE model with the damper can be due to the influence of the airbags decelerating the dummy. The airbags adds stiffness into the system, resulting in a steeper velocity plot that is closer to

the physical test data, as seen in the full scale FE model with the damper.

5.5 Advantages of the damper system for deceleration

The results obtained from the damper solution has proved to be a suitable alternate to the HC as the deceleration feature in the crash test setup. The adjustability factor of the HC has hindered conducting several tests with various loads and velocities. With dampers, a tunable deceleration feature, more tests can be conducted on different percentile dummies, which could strengthen the understanding of the performance of the airbags. It also gives the industry an opportunity to test more airbags of different concepts and parameters. The extended scope of this thesis work was to use the crash setup to conduct tests on the driver side airbags (DAB) as well. The results from this thesis work can help in designing the damper for a new load case, by mapping the acceleration and velocity plots for the new load case.

6 Conclusion

With a defined objective to replace the HC in the test setup, the damper system proposed is a good alternate for decelerating the sled. The damper was effective in recreating the HC's crash behaviour while also making the test setup reusable, customizable, and robust within the limited packing area. The proposed full scale CAE model with the damper, which was created by replacing the honeycomb, matches well with the test data results obtained from the physical tests. Due to time constraints, the validation phase using the physical damper in the test setup could not be performed.

The research conducted during the thesis can aid in tuning a new damper for future load requirements for the industry. The availability of multiple dampers on the market, as well as the industry's knowledge with installation and service, makes the damper more practicable than the other deceleration design options analyzed. Though the initial investment of an industrial damper can be high, it can used for several test loops over the years.

The proposed damper that could replicate the test data is a self-compensating damper that could be specific for one car with one load case. But a new damper can be designed and tuned for a new load case that the test rig should perform in the future. This could help in expanding the scope to conduct tests for driver side airbag or other NCAP net load cases.

The full scale CAE model with the damper had reduced the simulation time by 15% compared to the CAE model with the HC. This is achieved since the number of elements in the HC (58000) and anvil (26000) were reduced to a simple discrete damper and a spring element connected to a plate. A long term goal of validating the CAE model with the test setup could recreate the real time physics of the test setup. This well-built CAE model can assist in overcoming the expenses and time involved in physical tests in the future. Advanced CAE models could help in testing multiple airbags with different load cases with today's computational power.

References

[1] NHTSA. "Lives saved in 2017 by restraint use and minimum-drinking-age laws." (), [Online]. Available: https://crashstats.nhtsa.dot.gov/Api/Public/ViewPublication/812683. (accessed: 27-Apr-2022).

[2] C. J. (Kahane, "Lives saved by vehicle safety technologies and associated federal motor vehicle safety standards, 1960 to 2012 – passenger cars and ltvs – with reviews of 26 fmvss and the effectiveness of their associated safety technologies in reducing fatalities, injuries, and crashes." [Online]. Available: https://crashstats.nhtsa.dot.gov/Api/Public/ViewPublication/812069.pdf, (accessed: 27-Apr-2022).

[3] easy composites. [Online]. Available: https://www.easycomposites.co.uk/19mm-aluminium-honeycomb.

[4] IIHS, "Understanding Crash Crashes : It's basic physics," 2020, Accessed: April. 19, 2022. [Online]. Available: https://www.youtube.com/watch?v=2XKOzibVqJg.

[5] P. D. Bois et al., "Vehicle crashworthiness and occupant protection." [Online]. Available: https://www.roadsafellc.com/NCHRP22-24/Literature/Papers/Vehicle%20Crashworthiness%20and%20Occupant%20Protection(Book).pdf.

[6] Skybrary. [Online]. Available: https://skybrary.aero/articles/runway-arrestor-gear-systems.

[7] M. Kirpluks et al., "Modeling the effect of foam density and strain rate on the compressive response of polyurethane foams," 2, vol. 11, SAE International, 2018, pp. 131–138. [Online]. Available: https://www.jstor.org/stable/26556839 (visited on 05/26/2022).

[8] F. Billotto, M. Mirdamadi, and B. Pearson, "Design, application development, and launch of polyurethane foam systems in vehicle structures," Mar. 2003. DOI: 10.4271/2003-01-0333.

[9] E. A. Williams, G. Shaw, and M. Elahinia, "Control of an automotive shape memory alloy mirror actuator," Mechatronics, vol. 20, no. 5, pp. 527–534, 2010.

[10] H. Abuzied et al., "Usage of shape memory alloy actuators for large force active disassembly applications," Heliyon, vol. 6, no. 8, e04611, 2020.

[11] Ls-Dyna Support. [Online]. Available: https://www.dynasupport.com/howtos/general/consistent-units.

[12] Mithun Sridharan, "Pugh Matrix: How to use criteria in evaluating alternatives?," July.21, 2020, Accessed: April. 20, 2022. [Online]. Available: https://thinkinsights.net/consulting/pugh-matrix/.

[13] LS-DYNA®KEYWORD USER'S MANUAL, "Volume 1," English, Livermore Software Technology, July 17, 2020.

[14] The Physics Factbook. [Online]. Available: https://hypertextbook.com/facts/2005/steel.shtml.

[15] C. Moure-Guardiola et al., "Evaluation of combat helmet behavior under blunt impact," Applied Sciences, vol. 10, p. 8470, Nov. 2020. DOI: 10.3390/app10238470.

A APPENDIX

A.1 keycard for simple model

```
*KEYWORD
*NODE
$ total 2140 nodes were created
$     NID               Xcord               Ycord               zCord
          T Cons.  R cons.
        1                  0.                -15.                  0.
                  7       7
        2                350.                  0.                  0.
                  5       7
        3                  0.                 15.                  0.
                  7       7
        4                350.                -15.                  0.
                  5       7
$           .
$           .
$           .
$           .
*ELEMENT_DISCRETE
$       EID     PID    Node 1    Node 2         VID         S
             PF          Offset
        1       1       1         4                         0.
                 0                 0.
        2       4       3         5                         0.
                 0                 0.
*ELEMENT_SHELL
$ total 321 shell elements were created out of which only
    few are representaed
       18       3    1495    1497    1865    1868
       20       3    1502    1496    1303    1899
       21       3    1514    1851    1290    1852
$         .
$         .
$         .
```

```
$          .
*CONSTRAINED_EXTRA_NODES_NODE
$        PID         NID       IFLAG
             3           5           0
             3           4           0
*CONTACT_AUTOMATIC_SURFACE_TO_SURFACE_ID
$  ID          Type
1              *CONTACT_AUTOMATIC_SURFACE_TO_SURFACE
$       SSID        MSID       SSTYP       MSTYP
             5           3           3           3
                                                   0           0
$         FS          FD          DC          VC         VDC
           0.7         0.6                                     0

*PART
Damper Discrete Section
$        PID       SECID         MID                       GRAV
             1           1           3                          0
*SECTION_DISCRETE_TITLE
Damper Discrete Section
             1           0

*PART
Moving plate property
$        PID       SECID         MID       EOSID                 GRAV
          ADPOPT
             3           3           6                          0
                         0
*SECTION_SHELL_TITLE
Moving plate property
$        PID     ELFORM        SHRF         NIP       PROPT
             3           2          1.          2.          1.          0
                         0
$        T 1
           10.         10.         10.         10.
                                                  0.
*PART
```

```
Spring Discrete Section
         4         4         4                                   0
*SECTION_DISCRETE_TITLE
spring Discrete Section
         4         0

*PART
Sled plate Property
         5         5         5                                   0
                   0
*SECTION_SHELL_TITLE
Sled plate Property
         5         2        1.        2.        1.              0
                   0
        5.        5.        5.        5.
                                      0.
*BOUNDARY_SPC_NODE_ID
         1Damper Fixed End
$                            Constrained all Dofs
         3                   1         1         1         1
                   1         1
         3Spring Fixed End
$                            Constrained all Dofs
         1                   1         1         1         1
                   1         1
         2Spring Plate End
$                            Constrained all Dofs except
    transalational x
         5                   0         1         1         1
                   1         1
         4Damper Plate End
$                            Constrained all Dofs except
    transalational x
         4                   0         1         1         1
                   1         1
*INITIAL_VELOCITY_GENERATION
$       PID       STYP      OMEGA        VX        VY        VZ
```

```
         IVATN      ICID
             5         2         0.     -11.3          0.         0.
                   0         0
$
            0.        0.         0.         0.         0.         0.
                   0         0
*MAT_DAMPER_NONLINEAR_VISCOUS_TITLE
MAT_S05 Damper
$       MID      LCDR
          3         1
*MAT_SPRING_ELASTIC_TITLE
MAT_s01 Spring
$       MID         K
          4      0.09
*MAT_PIECEWISE_LINEAR_PLASTICITY_TITLE
impactor material property
$       MID        RO          E        PR      SIGY      ETAN
       FAIL      TDEL
          5 0.0031407       210.       0.3      0.35         0.
             1.E20        0.
            0.        0.                                  0.
            0.        0.         0.         0.         0.         0.
                0.        0.
            0.        0.         0.         0.         0.         0.
                0.        0.
*MAT_RIGID_TITLE
moving plate material
$       MID        RO          E        PR      SIGY      ETAN
       FAIL      TDEL
          6   7.85E-6       210.       0.3         0.         0.
                 0.
           1.0        5.         7.
            0.        0.         0.         0.         0.         0.
*DEFINE_CURVE_TITLE
Damper Load Curve
$       PID      SIDR        SFA       SFO      OFFA      OFFO
     DATTYP     LCINT
```

```
         1         0        1.        1.        0.        0.
                       0         0
$             Xcord                 Ycord
             -12.                 -23.5
              -1.                  -08.
               0.                   0.
```